# Arabian Journal of Chemical and Environmental Research Vol. 11 Issue 2 (2024) 110–136



## Remediation of Radon from Groundwater Using Corncob Activated Carbon in Pour-Through Filter System

Rebecca A. Olaoye<sup>1,2</sup>, Aderonke O. Abiola<sup>1,2</sup>, Monsusru, O. Dauda<sup>2,3,5</sup> and Abass O. Alade<sup>2,3,4,5</sup>\*

- <sup>1</sup> Department of Civil Engineering, Faculty of Engineering, Ladoke Akintola University of Technology, Ogbomoso, Nigeria <sup>2</sup> LAUTECH SDG 6 Research Cluster (LSDGRC-6), Ladoke Akintola University of Technology, Ogbomoso, Nigeria
  - <sup>3</sup> Department of Chemical Engineering, Faculty of Engineering, Ladoke Akintola University of Technology, Ogbomoso, Nigeria
  - <sup>4</sup> Bioenvironmental, Water and Engineering Research Group, (BWERG), Ladoke Akintola University of Technology, Ogbomoso, Nigeria

Received 03 Nov 2024, Revised 22 Dec 2024, Accepted 24 Dec 2024

Cited as: Rebecca A. Olaoye, Aderonke O. Abiola, Monsusru, O. Dauda, and Abass O. Alade (2024) Remediation of Radon from Groundwater Using Corncob Activated Carbon in Pour-Through Filter System, Arab. J. Chem. Environ. Res. 11(2), 110-136

#### **Abstract**

The potency of Corncob Activated Carbon (CCAC) for the remediation of radon in groundwater via a pourthrough system was investigated. Corncob samples were carbonized (400-600 °C) and activated with H<sub>3</sub>PO<sub>4</sub> for 24 h. The surface chemistry and morphology of the CCACs were characterized using Fourier Transform Infrared (FTIR) and Scanning Electronic Microscopy (SEM). Groundwater samples containing Radon were treated with the CCACs developed through the adsorption technique in a cylindrical plastic Pour-Through Filter Bed System. The radon concentrations were analysed using Professional Electronic Radon Detector (RAD-7). The FTIR spectra analysis of CCACs obtained at 400 °C (CCAC400), 500 °C (CCAC500) and 600 °C (CCAC600) showed the presence of O-H, C-H, C=O, C-O, C-OH, C-Br, C=C and C-F functional groups on their surfaces, while the SEM images indicate the presence of large hollows on the CCAC samples. The Groundwater sample has a radon concentration of 20.06 Bq/L, pH (6.6), TDS (1.75 mS/cm), and EC (1269 ppm). The CCAC600 had the maximum reduction of> 85% at 60 mins and the adsorption data obtained fitted to pseudo-second-order kinetic model II and Webber-Morris diffusion model. Corncob exhibited potency as an effective biomass for the treatment of radon-polluted wastewater via an adsorption treatment technique.

Keywords: Adsorption, Corncob, Diffusion, Kinetic, Pour-through.

\*Corresponding author.

E-mail address: aoalade@latech.edu.ng

ISSN: 2458-6544 © 2024; www.mocedes.org. All rights reserved.

<sup>&</sup>lt;sup>5</sup> Science and Engineering Research Group (SAERG), Ladoke Akintola University of Technology, Ogbomoso, Nigeria Email raolaoye@lautech.edu.ng; abiolaaderonketosin@gmail.com; monsuruodauda@gmail.com; aoalade@latech.edu.ng\*

#### 1. Introduction

One of the main sources of exposure of humans to naturally occurring radiation is radon gas. Radon (Rn-222) is a radioactive noble gas soluble in water, cannot be seen, smelled, or tasted and has a density that is 7.5 times higher than that of air. Radon gas comes from the natural decay series of Uranium-238 in the rocks and soil with a half-life of 4.5x10<sup>9</sup> years (Mustafa & Daniel, 2009). Uranium levels vary on Earth since certain types of rocks and soils such as granite, uranium-enriched phosphatic rocks, and shales, contain more uranium than others (Muikku *et al.*, 2007). Uranium breaks down into Radium (Ra-226) and radon is the decay product of radium. Radon comes in a variety of isotopes, but only Radon-222 is of importance because the other isotopes have relatively short half-lives (Appleton, 2007). The half-life of radon-222 is 3.82 days and decays within hours to form short-lived radionuclides and other radioactive progeny with the release of alpha and beta emissions. The Molecular Weight, Boiling Point, Melting Point, Solubility in Water, Air Diffusion Coefficient and Water Diffusion Coefficient of radon are 222 gm/M, 211 K(-62°C), 202 K(-71°C, 230 cm³/L @ 20°C, 1.2X10-5 m²Sec-1 and 1.2 X 10-5 m² Sec-1, respectively (USEPA, 1999). The movement of Radon from its source in rocks and soil through voids and fractures results in its dissolution in groundwater.

The potential hazard of radon gas at elevated concentrations in groundwater has been a global concern due to its devastating health effects. Ingestion of radon in water is associated with an increased risk of tumors of several internal organs, primarily the stomach (EPA, 1999; Arora et al., 2011). According to a National Academy of Science research, radon in drinking water causes around 168 cancer-related deaths each year, with roughly 89 percent of lung cancer caused by breathing radon emitted into the indoor air from water and 11 percent caused by swallowing radon-contaminated water. Globally groundwater is often the preferred source of water supply because of its reliability compared to surface water (Guppy et al., 2018) and it is a major source of water for drinking and other domestic purposes in most developing countries due to lack of access to water from the conventional water mains (Olaoye, et al., 2018; Danert & Healy, 2021; Olaoye, et al., 2021). It has been reported that radon activity in groundwater resources is heavily dependent on the area's geology (Seminsky & Seminsky, 2016). The variation of radon concentration in groundwater is influenced by several factors such as the presence of shear zones, degree of metamorphism; basement complex with granite as the most extensive unit, soil porosity, uranium mineralization, infiltration of surface water into aquifer among others (Choubey, et al., 2001; Idriss, et al., 2011). The concentration of radon in groundwater should be monitored and kept within the permissible level before consumption.

Two days of water storage can reduce about 30% of the initial mass, due to radon's short half-life, and radioactivity of radon in water. However, in most developing countries with excessive radon in the groundwater, the water is consumed almost immediately without having to wait for half-life, this is

particularly the case in most study areas where radon is excessive in groundwater. Therefore, there is a need for an immediate low-cost and sustainable technique for the removal of radon in groundwater before consumption.

Several technologies have been employed for the removal of radon in water. These techniques were broadly classified into aeration, granular activated carbon (GAC) and other simple combination techniques. However, most of these methods suffered from some drawbacks such as high capital and operational costs, regeneration costs, and residual disposal. The major drawback of aeration techniques is that they transmit radon pollution from water to air, thereby causing air contamination hazards and aeration is often not sufficient for removing radon from drinking water; it should be supported with the adsorption method (Ghernaout, 2019). Several studies have been carried out to determine the radon concentration in water. Lowry & Lowry 1988 in a study in the US on the need for a new approach and developments for the removal of radon emphasized the limitation of the aeration method for radon remediation.

Idriss et al., (2011 conducted a study to measure and map radon concentration in different wells used for the water supply network of Khartoum State and reported that some of the wells had radon concentration values below the permissible EPA standard while some were above the permissible level. Alabdula'aly & Maghrawy, (2011) compared different granular activated carbons for the removal of medium-level radon in water and reported different removal efficiencies. Yusuf, (2019) assessed the radon exposure in hand-pumped groundwater in Ogbomoso and came up with radon concentrations between 11.74 and 209.87Bq/L which is above the permissible concentration level of 11.1 Bq/L set by USEPA 1999 and other regulatory bodies while Oni et al. 2016 conducted a study in Ado Ekiti, and revealed that the radon content in groundwater samples was higher than the USEPA's maximum level. (Amodu et al., 2020) investigated the radiological risk of radon in borehole water in Ede and its environs and concluded that hand-pumped wells in the study area pose a high radiological risk over time, requiring further investigation to ensure the safety of the local population.

Site-specific studies are necessary to identify the most feasible, economical and efficient methods for the particular location where radon in groundwater is to be removed. Adsorption remains the most plausible and feasible alternative for the treatment of polluted water with radon (Sabino *et al.*, 2016). Due to the high cost of conventional preparation (Rao *et al.*, 2009) and the irreversible nature of adsorption, the usage of activated carbon is limited. Thus, a need for a low-cost adsorbent that will possess all the properties of synthetic activated carbon. Previous research on the use of agricultural leftovers, such as rice and wheat husks, has yielded promising results (Qui, *et al.*, 2008; Rao, *et al.*, 2009; Olaoye, *et al.*, 2018; N'diaye *et al.*, 2022), groundnut shells (Malik, *et al.*, 2007) and corncob (Anih,

2020) as raw materials for activated carbon production showed satisfactory success. The adsorption process takes place when the radon molecules pass from the water to the surface of the GAC. Radon sorbs at the interface between the water and the carbon.

The current study looks at the usage of activated carbon made from discarded corncob to reduce or eliminate radon from water. Corncobs are a significant source of solid waste in the agriculture sector. Every year, millions of tons of corncob are discarded into the environment, leading to solid waste nuisance and possible blockage of waterways, particularly after rain (Amuda, et al., 2014). Excellent sorption properties of activated carbon obtained from corncob for gas and liquid pollutants have been reported (Justyna, 2012). Corncob activated with phosphoric acid was reported to be more effective for dye wastewater treatment than corncob activated with potassium hydroxide and zinc chloride solutions. (Ezeh, et al., 2019) reported effective adsorption of cadmium II ions from aqueous solution using corncob-activated carbon while (Zhou, et al., 2018) observed higher pollutant removal efficiency for smaller particle-sized activated charcoal than for bigger size particles. In this study carbon from corncob was activated with phosphoric acid (H<sub>3</sub>PO<sub>4</sub>) to remediate radon from groundwater in an economic pourthrough filter system. Subjecting such agricultural material to high heat and pressure increases its surface area and activating it improves its ability to absorb polluting substances; both organic and dissolved gases from the groundwater. Pour-through systems are usually granular bed or candle filters for contaminant removal or reduction. Water is poured into the units and goes through the filtering medium by gravity. Sometimes a pump is used to increase the filtration rate. Pour-through models are inexpensive and the simplest type of activated carbon filter in which water is poured through the carbon and collected in a container (Dvorak & Skipton, 2013).

#### 2 Materials and methods

#### 2.1 Materials and reagents

The main material used in this work is corncob which was bought from the Arada market (8°06'46.6''N4°14'48.5''E) in Ogbomoso in Oyo State. The reagents used include Sodium Hydroxide (NaOH), orthophosphoric acid (H<sub>3</sub>PO<sub>4</sub>), distilled water, plastic tray, foil paper and mesh cloth. All reagents used were of analytical grade and sourced from The Bioenvironmental, Water and Engineering Research Group (BWERG) Laboratory, in Chemical Engineering Department, Ladoke Akintola University of Technology, Nigeria.

## 2.2 The Study Area and Sampling Location

Ikoyi-Ile is found in Oriire Local Government Area of Oyo State, which was created in 1989 and has its administrative headquarters in the town of Ikoyi. It is bordered by Atiba, Olorunsogo and Surulere

LGAs. The LGA counts as one of the largest LGAs of the State both in areas and in population as shown in Figure 1. The study area resides on the African crystalline rocks, which are chiefly composed of metasedimentary, igneous and meta-igneous rocks (Sunmonu, et al., 2012; Adagunodo, et al., 2013). The rocks of Ogbomoso are an integral part of the Proterozoic Schist belt (Sunmonu, et al., 2013), which developed towards the western half of Nigeria. The lithological units in Ogbomoso include granitegneiss, banded gneiss and quartzite. Augen and agmatitic gneisses are also present in the study area. The quartzite occurs as elongated ridges, which trends in NW-SE orientation. The quartzites are observed as Schistose, which dominates the southern region, while granite gneisses cover the northeastern region of the town (Adabanija et al., 2014).

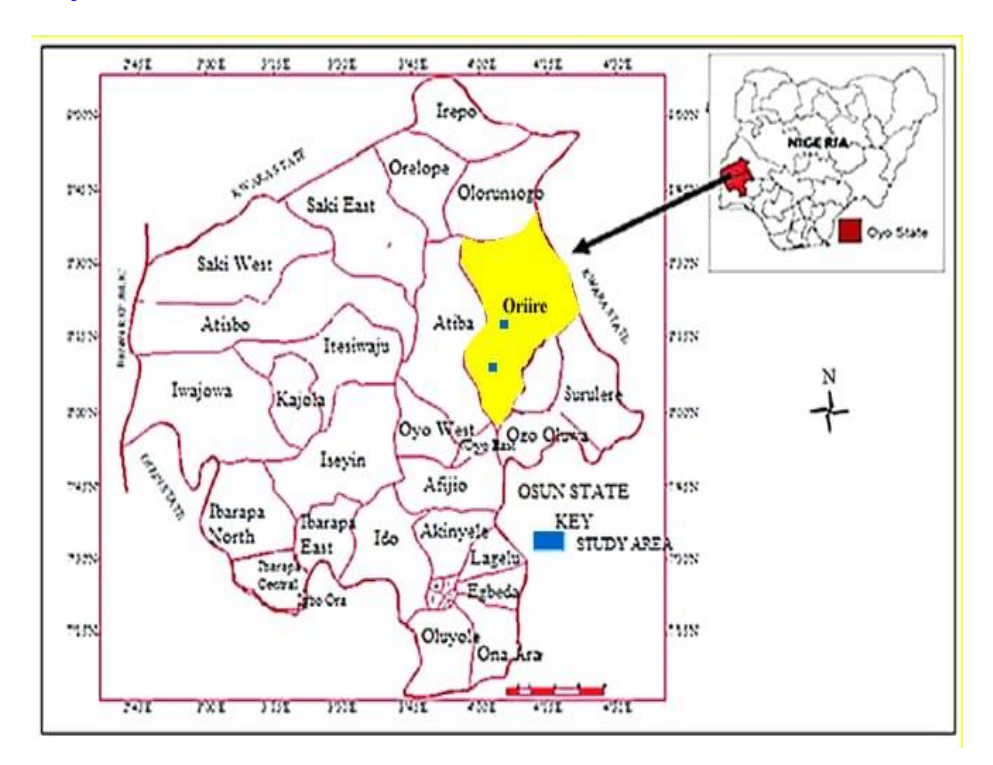


Figure 1: Map of Oyo State showing Oriire Local Government

Seven source points were considered in the Ikoyi area of Orire local government. Water samples were taken from a hand-pumped well at the front of the palace (8°14'58" N 4°10'39" E), Ile Ojude (8°14'42" N 4°10'5" E), local government compound, Ile Olomoba, Omo Ola Aluminium, Health Centre (8°14'42" N 4°10'29" E) and Basic school (8°14'42" N 4°10'32" E). Basis school came out as the source with the highest radon concentration which is above the Maximum Contaminant Level (MCL) of 11.1Bq/L set by USEPA 1999 and other regulatory bodies (Table 2).

## 2.3 Adsorbent preparation

The corncob sample collected was washed thoroughly, to remove dirt from its surface and then sundried before being crushed and ground with a grinder into granules. The sample was carbonized in the Gollenkamp muffle furnace at 400, 500 and 600 °C for 1 h, separately. The carbonized samples were cooled in a desiccator to avoid the formation of ashes and then reweighed and labeled appropriately. The carbon yield from each was calculated by Eqn. 1 (Fapetu, 2000). The carbonized corncob was further ground and sieved into 1.0 mm, 2.0 mm and 2.8 mm for each carbonization temperature. The carbonized samples were activated with 0.3 M Orthophosphoric acid (H<sub>3</sub>PO<sub>4</sub>) at a ratio of 1:1 w:v of char to H<sub>3</sub>PO<sub>4</sub> solution. The mixture was agitated for 30 mins, covered with foil paper and left for 24 h after which it was filtered. The residue (activated corncob) was washed with distilled water and further neutralized with 0.1M NaOH to pH 6.9-7.1. The Corncob Activated Carbon (CCAC) developed was oven-dried at 110 °C to constant moisture content and then kept in a closed and labeled container for the adsorption experiment:

$$Y_{ch} = \frac{W_{ch}}{W_0} X 100 \tag{1}$$

where  $W_{\text{ch}}$  =Weight of the carbon retrieved from the furnace, and  $W_{\text{o}}$  = Dried weight of the raw sample.

### 2.3 Characterization of activated carbon

The physicochemical and surface characterization of the CCAC developed were carried out to determine the properties of the activated carbon produced.

### 2.3.1 Proximate Analysis

## 2.3.1.1 Determination of moisture content

The corncob sample (5 g) was oven-dried at 105 °C for 24 h and then cooled in a desiccator, to prevent any moisture uptake from the atmosphere and before reweighing. The percentage of moisture removed was evaluated using Eqn. 2 (Jeandson, Roberta, Marcio, & Dênia, 2018):

Moisture content = 
$$\frac{A-B}{A}$$
 X 100% (2)

#### 2.3.1.2 Determination of ash content

The corncob sample (2.5 g) was ashed in a muffle furnace at 760 °C for 1.5 h and the resulting ash content was cooled in a desiccator before being reweighed. The amount of ash was deduced according to Eqn. 3 (Feng, Yang, & Chu, 2015):

$$\%Ash = \frac{\text{Weight of ash}}{\text{Weight of original sample}} x \ 100 \ \ (3)$$

#### 2.3.1.3 Fixed carbon determination

The fixed carbon (FC) content of the corncob sample was deduced from Eqn 4, based on the assumption that the sulphur content of the sample is negligible (Fapetu, 2000):

$$FC = \frac{(CY - MC - VC - AC)}{CY} (\%) \tag{4}$$

where CY = carbon yield (%), MC = moisture content (%), VC = volatile content (%), and AC = Ash content (%).

## 2.3.1.4 Crude fibre determination

The corncob sample (20 g) was defatted with diethyl ether for 8 h and boiled under reflux for 30 mins with 200 ml of 1.25% H<sub>2</sub>SO<sub>4</sub>. The mixture was filtered and the residue was washed with boiling water to remove the acid content before being treated with 200 ml of 1.25% NaOH by boiling in a round-bottom flask for 30 mins and then filtered. It was oven-dried at 105 °C, cooled in a desiccator, reweighed and then ashed in a muffle furnace at 600 °C for 2 h. It was cooled in a desiccator and reweighed, then the crude fibre content was determined from Eqn 5:

% Fibre = 
$$\frac{\text{weight of fibre}}{\text{weight of original sample}} X100 (5)$$

#### 2.3.2 Analytical characterization

## 2.3.2.1 Surface characterization

The Fourier Transform Infrared (FTIR) spectroscopic analysis of the raw and activated carbon samples produced was performed using BUCK FTIR ((M530 SPEC) to get information about the characteristic functional groups on the surfaces of the samples. The samples were prepared with 100 mg of KBr which was compressed into a thin pellet for 5 min and then placed in the sample holder. The spectra were measured from 4000 to 400 cm<sup>-1</sup> and the appropriate reading was displayed on the screen and then copied (Okeowo *et al.*, 2020).

## 2.3.2.2 Morphology characterization

The morphology characteristics of the raw and activated carbon samples produced were performed using Scanning Electron Microscope SEM (Aspex 3020 model, FEI, PSEM 2), based on the manufacturer's protocol.

## 2.4 Measurement of Radon in Groundwater Sample

The water samples from the hand-pumped borehole from the study location were collected in a precleaned 25 litres black plastic container (PWS, 2019). Agitation of the sample was avoided to prevent losses of radon. The water was made to flow slowly and steadily into the sampling plastic through a hose, which allowed the container to be filled bottom-up, inside the bottle. The container was covered tightly to prevent leakage or spill during transportation to the laboratory. The desired analysis was carried out within 2 h of arrival at the laboratory.

The samples were assayed for radon using a calibrated portable electronic radon monitoring device (RAD 7, Durridge, USA) (Figure 2a) which is capable of measuring radon in water and soil. The RAD7 is a sniffer that uses the 3-minute alpha decay of the radon daughter, without interference from other radiations and the instantaneous alpha decay of a thoron daughter. The device determines the radon concentration in water within 10 mins which is far lower than the half-life (3.82 days) of radon, hence the choice of this device.

The radon detector was coupled with a bubbling kit to measure the radon concentration in water samples. WAT 250 protocol and grab mode were used for radon measurements in the water samples (Figure 2b). Initially, the inbuilt pump of RAD7 runs automatically for 5 mins to aerate the sample and deliver the degassed radon to the RAD7 measuring chamber. The pump then stops automatically and the system waits for another 5 mins interval to start counting, after which the data along with the respective bar charts and cumulative spectra of each sample are printed out on the printer attached to the instrument.

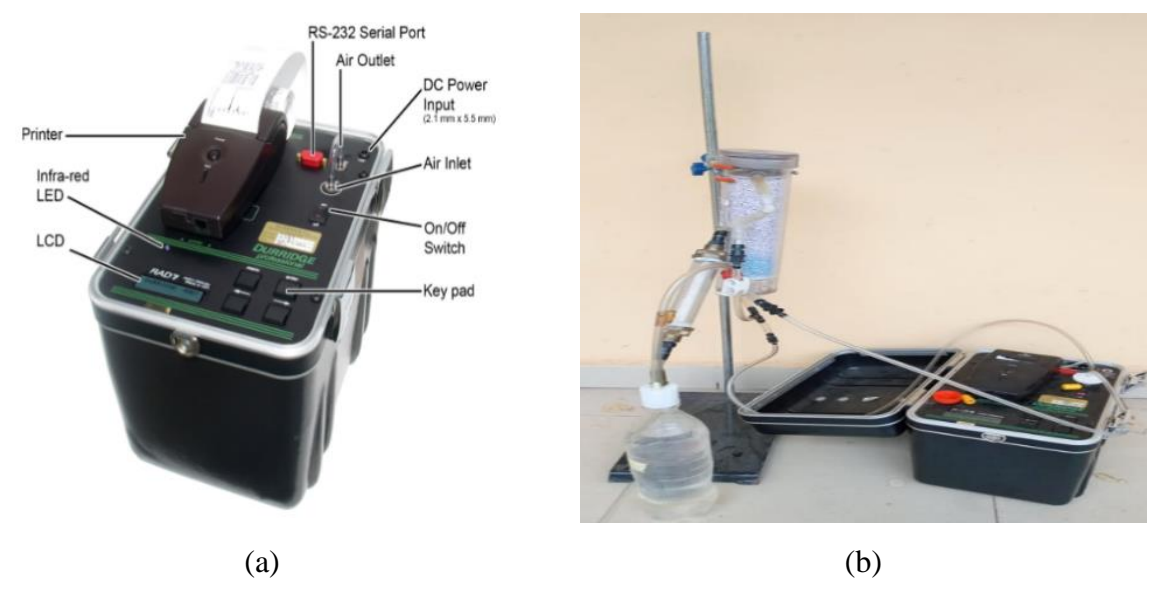


**Figure 2:** (a) RAD7 Professional Electronic Radon Detector and (b) RAD7 setup for water sample testing

Source: RAD7 Durridge Electronic Radon Detector User Manual

## 2.5 Groundwater characterization

The physicochemical parameters of the groundwater analysed were pH, Total Dissolved Solids (TDS) and Electrical Conductivity (EC) using an EC/TDS tester (Adwa AD31 waterproof EC/TDS Testers), according to the manufacturer specifications.

## 2.6 Pour-through filter bed setup

The Pour-through filter bed was made of a plastic container (18 and 16 cm, top and bottom diameter) having a mesh at the bottom (Bryant & Tettehh-Narh, 2015), and an outlet pipe, with an attached manual

flow meter at the bottom of the container. The container used was kept at 1.8 m elevation. The CCAC samples with sizes of 2.8 mm (75 g), 2.0 mm (75 g) and 1.0 mm (75 g) were packed in succession on top of one another. The groundwater sample (2000 ml) with elevated radon was released into the pourthrough filter bed and the container was covered with a tight lid to avoid exposure to the air. A 20 mins retention time was allowed before running the water at the flow rate of 1.5 mL/s and sampling was done at 10 mins intervals until 60 mins. The treated water samples were assessed for radon concentration and other water characteristics. The adsorption capacity and removal efficiency of the CCAC400, CCAC500 and CCAC600 were determined according to Eqns 6 and 7 respectively, while the adsorption capacity(qt) for time was determined according to Eqn 8 for concentration (Ct) removed at each time:

$$q_t = \frac{(C_o - C_t)}{m} V \tag{6}$$

$$RE = \frac{c_o - c_e}{c_o} X 100 \tag{7}$$

where  $C_o$  = initial concentration of radon,  $C_t$  = concentration of radon after adsorption at time t, m = mass of CCAC used and V = volume of water in the pour-through filter bed.

## 2.6 Adsorption Kinetics Studies

The data obtained for time were used to evaluate the parameters of the selected adsorption kinetic models.

#### 2.6.1 Pseudo-first-order Kinetics

The values of  $K_1$  and  $q_e$  of the pseudo-first-order equation (Eqn 9) were calculated from the slope and the intercept of the plots of the  $\log(q_e - q_t)$  against t, respectively (Amole *et al.*, 2021).

$$\log(q_e - q_t) = \log q_e - \frac{\kappa_1}{2.303}t \tag{9}$$

where  $q_e$ = amounts of the radon adsorbed (mg/g) at equilibrium,  $q_t$  = amounts of the radon adsorbed (mg/g) at time t (min), respectively, and  $K_1$  = rate constant of adsorption (min<sup>-1</sup>).

#### 2.6.2 Pseudo second order kinetics

The values of  $q_e$  and  $K_2$  of the pseudo second-order kinetics equation (Eqns 10-14) were obtained from the slope and the intercept of the straight-line plots (Elmorsi *et al.*, 2014).

Model I 
$$\frac{1}{a_0 - a_t} = \frac{1}{a_0} + k_2 t$$
 (10)

Model II 
$$\frac{t}{q_t} = \frac{1}{K_2 q_e^2} + \frac{1}{q_e} t$$
 (11)

Model III 
$$\frac{1}{q_t} = \frac{1}{q_e} + \frac{1}{k_2 q_e^2} \frac{1}{t}$$
 (12)

Model IV 
$$q_t = \frac{q_t}{k_2 q_e^2} \cdot \frac{1}{t} + q_e$$
 (13)

Model V 
$$\frac{q_t}{t} = k_2 q_e^2 - k_2 q_e q_t$$
 (14)

where  $K_2$  (g/mg/min) = pseudo second order kinetic parameter.

#### 2.6.3 Elovich model

The Elovich kinetic model constants ( $\alpha$  and  $\beta$ ) were evaluated from the linear curve of  $q_t$  versus  $\ln t$  (Eqn 15):

$$q_t = \frac{1}{\beta} \ln(\alpha \beta) + \frac{1}{\beta} \ln t \tag{15}$$

where  $\alpha$  = initial adsorption rate in mg/g.min,  $\beta$  = rate of surface coverage and the activation energy of adsorption.

## 2.7 Error Analysis

The sum of Square of the Errors (SSE), Sum of the Absolute Errors (SAE) is expressed and Average Relative Error (ARE) are expressed in Eqns 16-18 (Kundu & Gupta, 2006).

$$SSE = \sum_{i=1}^{n} (q_{e \, est} - q_{e \, exp})_{i}^{2} \tag{16}$$

$$SAE = \sum_{i=1}^{n} \left| q_{e \, exp} - q_{e \, est} \right|_{i} \tag{17}$$

$$ARE = \frac{100}{n} \sum_{i=1}^{n} \left[ \frac{q_{e\,est} - q_{e\,exp}}{q_{e\,exp}} \right]_{i}$$
 (18)

where,  $q_{e(estm)}$  = estimated value of the equilibrium adsorbate solid concentration in the solid phase (mg/g),  $q_{e(exp)}$  = experimental value of the equilibrium adsorbate solid concentration in the solid phase (mg/g) and n = number of the data point.

#### 2.8 Diffusion Models

Adsorption processes could be either physically or chemically controlled, based on liquid film diffusion which involves the mass transfer rate process or intraparticle diffusion.

## 2.8.1 Intra-particle diffusion (Webber-Morris) model

The Webber-Morris is a rate-determining model (Eqn 19) and the intraparticle diffusion constants were evaluated from the plot of  $q_t$  vs  $\sqrt{t}$ .

$$qt = k_{id}t^{0.5} + C (19)$$

where  $K_{id}$  = the intraparticle diffusion rate constant (mg/min<sup>1/2</sup>), and C = the constant for the thickness of the boundary layer (mg/g).

## 2.8.2 Dumwald-Wagner diffusion model

The Dumwald-Wagner diffusion is expressed in Eqn 20 and the plot of  $log(1-F^2)$  vs t gave a linear plot from which the diffusion rate constant (K) was evaluated.

$$\log(1 - F^2) = -\left(\frac{K}{2.303}\right) X t \tag{20}$$

where  $F = \frac{q_t}{q_e}$ , K = the diffusion rate constant (min<sup>-1</sup>),  $q_t =$  the adsorption capacity (mg/g) at time t,  $q_e =$  the adsorption capacity (mg/g) at equilibrium.

## 2.8.3 McKay film diffusion mass transfer

The McKay film diffusion (Eqn 21) relates mass transfer to film diffusion and it is represented as the plot of ln(1-F) against a linear plot in which the value for the rate constant of the process,

$$ln (1 - F) = -K_m t$$
(21)

where K<sub>m</sub> (min<sup>-1</sup>), is the McKay film diffusion rate constant

#### 3. Results and Discussion

## 3.1 Characteristics of Corncob Adsorbent Developed

#### 3.1.1 Proximate analysis

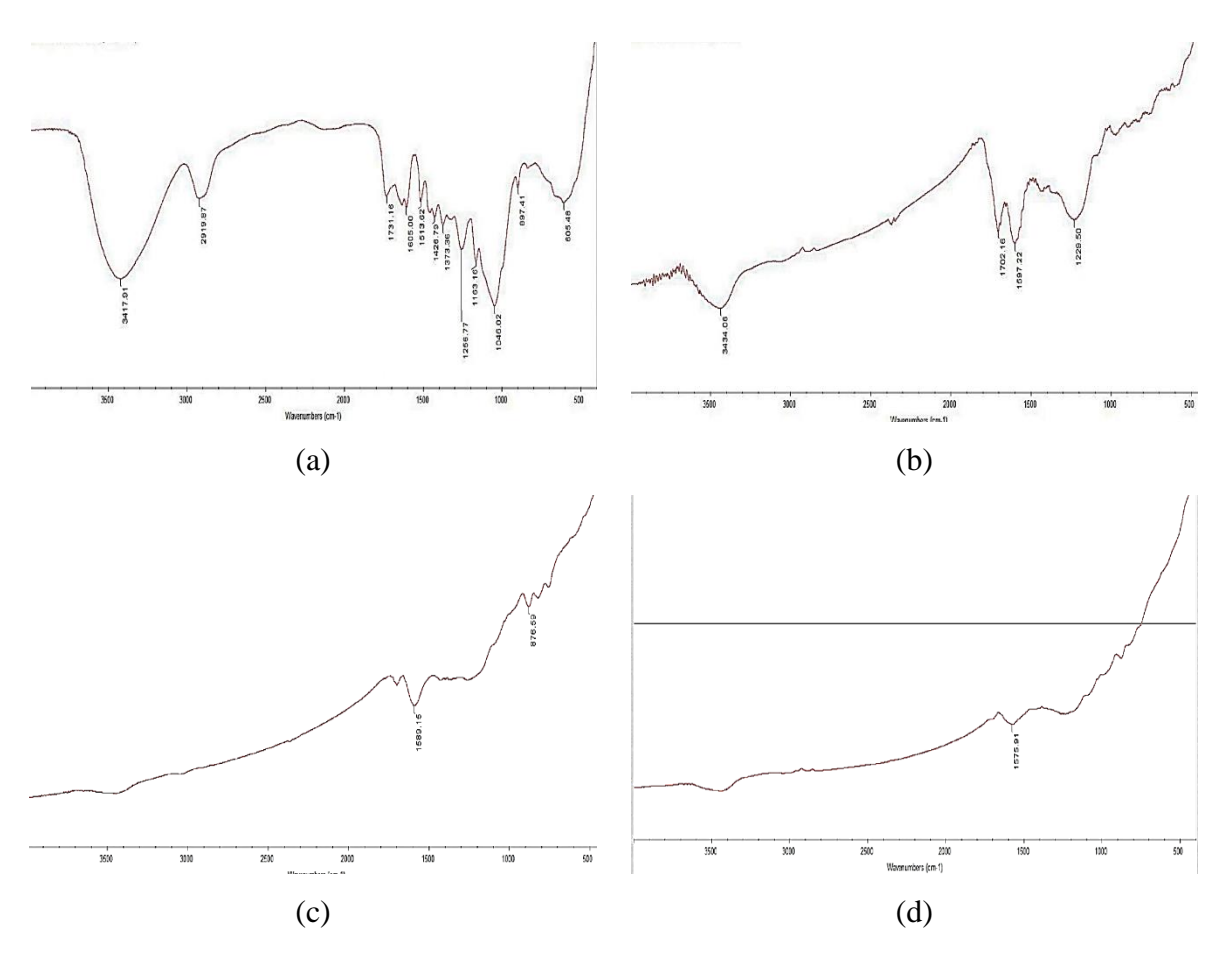
The moisture content of the raw corncob was 6.1% which is lesser than the 6.5% obtained by (Igwegbe et al., 2021), but compared very well with 5.8 and 6.0% reported (Akuso, et al., 2019) and (Abubakar, et al., 2016), respectively. The ash content of 2.42 % obtained is slightly lower than 2.5 and 3.9 % reported by (Abubakar, et al., 2016) and (Akuso, et al., 2019), respectively. Ash content is related to the amount of volatile matter that can be released as the carbonization temperature increases. Less ash content of activated carbon facilitates higher adsorption capacity (Yang, et al., 2010). The crude fibre of 15% obtained is similar to the value (14%) obtained by (Akuso, et al., 2019). The carbon yield of 27.85 %, 26.16 % and 17.56 % was obtained for CCAC400, CCAC500 and CCAC600 respectively (Table 4). The carbon yield decreased as the carbonization temperature increased and this indicates that the more volatile components of the corncob were released at elevated temperatures.

Table 4: Proximate analysis of raw corncob

Pro	Property (wt. %)  References		References
Moisture content	Ash content	Crude fibre	References
6.0	2.50	33.3	Abubakar et al., (2016)
5.8	3.90	14.0	Akuso et al., (2019)
6.1	2.42	15.0	This study

## 3.1.2 FTIR characteristics

The FTIR spectra of corncob before carbonization and after activation at 400, 500 and 600 °C (Figures 3a-d) and their comparable features of adsorption bands (Table 5) revealed the existence of different functional groups with disappearance, reduction, or broadening of the peaks after the acid activation process. The shifts in bands and changes in wavelength between the raw sample and the activated samples indicate that chemical transformation took place during the chemical activation and/or carbonization. The stretched bandwidth observed at 3417.91 cm<sup>-1</sup> on the raw sample (Figure 3) was assigned to O-H stretching vibration of hydroxyl groups such as hydrogen bonding. The aliphatic C-H stretch was assigned to the band seen at 2919.87 cm<sup>-1</sup>. Carboxylic C=O stretching vibrations are attributed to lactone, ketone and carboxylic anhydride. The oxygen group C-O band at 1256.77 cm<sup>-1</sup>. C-OH stretching, C-Br, and C-HC-O disappeared in the carbonized activated samples, and this shows a thermal instability of the functional groups. There were appearances of C=C and C-F stretching at the CCAC400 at 1597.22 and 1229.50 cm<sup>-1</sup>, respectively (Fig. 3b). Only C=C aromatic rings were retained on the CCAC500 and CCAC600 (Figure 3c-d).



**Figure 3:** FTIR Spectra of (a) raw corncob as well as activated carbonized corncob at (b) 400 °C, (c) 500 °C, and (d) 600 °C

**Table 5:** FTIR analysis

Sample	Frequency (cm <sup>-1</sup> )	Functional group
Raw Corncob	3417.91	O-H Stretching
	2919.87	C-H Stretching
	1731.16	C=O Stretching
	1256.77	C-O Stretching
	1046.02	C-OH Stretching
	605.48	C-Br Stretching
CCAC400	3434.06	O-H Stretch
	1702.16	C=O Stretch
	1597.22	C=C Stretch
	1229.50	C-F Stretch
CCAC500	1589.15	C=C Stretch
	876.59	C=C bending
CCAC600	1575.91	C=C Stretch

CCAC – Corncob Activated Carbon

## 3.1.3 Morphology Characteristics

SEM images of the best-activated carbon samples produced showed the surface texture with cavities and openings found on the surfaces which facilitate pore diffusion of adsorbate during the sorption process (Figure 4a-c). The CCAC500 has the widest cavity sizes, while CCAC400 had the smallest and this may be attributed to the effects of the activation and high carbonisation temperature which are responsible for the breaking down of the lignocellulosic materials and further volatilization of the embedded volatile compounds (Hu, *et al.*, 2018).

## 2.3 Physicochemical Characteristics of Water Samples

The pH of the raw groundwater sample was 6.6 (Figure 5a) and this suggests that the groundwater samples are weakly acidic. However, the pH of the treated groundwater samples at each time is 6.5 which is constant for all the three activated samples produced. This indicated about 1.5 % reduction, thus suggesting that the use of CCAC produced will not alter the pH of the groundwater sample adversely. Although, the pH of most drinking water lies within the range of 6.5-8.5 (WHO, 2008) (Table 6). The initial TDS of the raw water sample was 1.75 mS/cm which increased to 1.99-2.27, 2.37-3.26 and 2.11-2.24 ppm for CCAC400, CCAC500 and CCAC600, respectively, (Figure 5b) at a retention time range of 20-60 mins (Table 6). This may be due to the desolation of some micro solutes in the activated carbon produced.

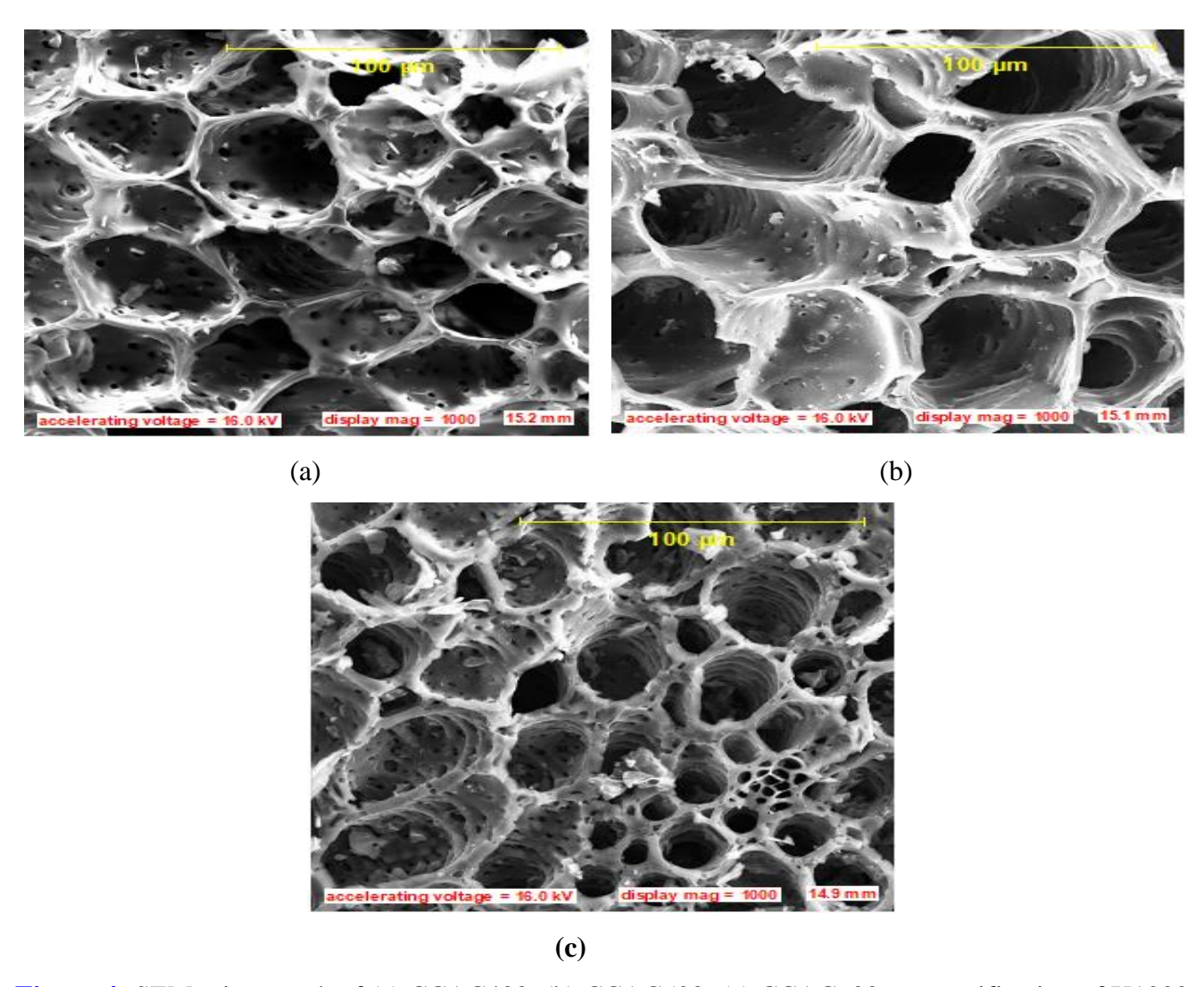
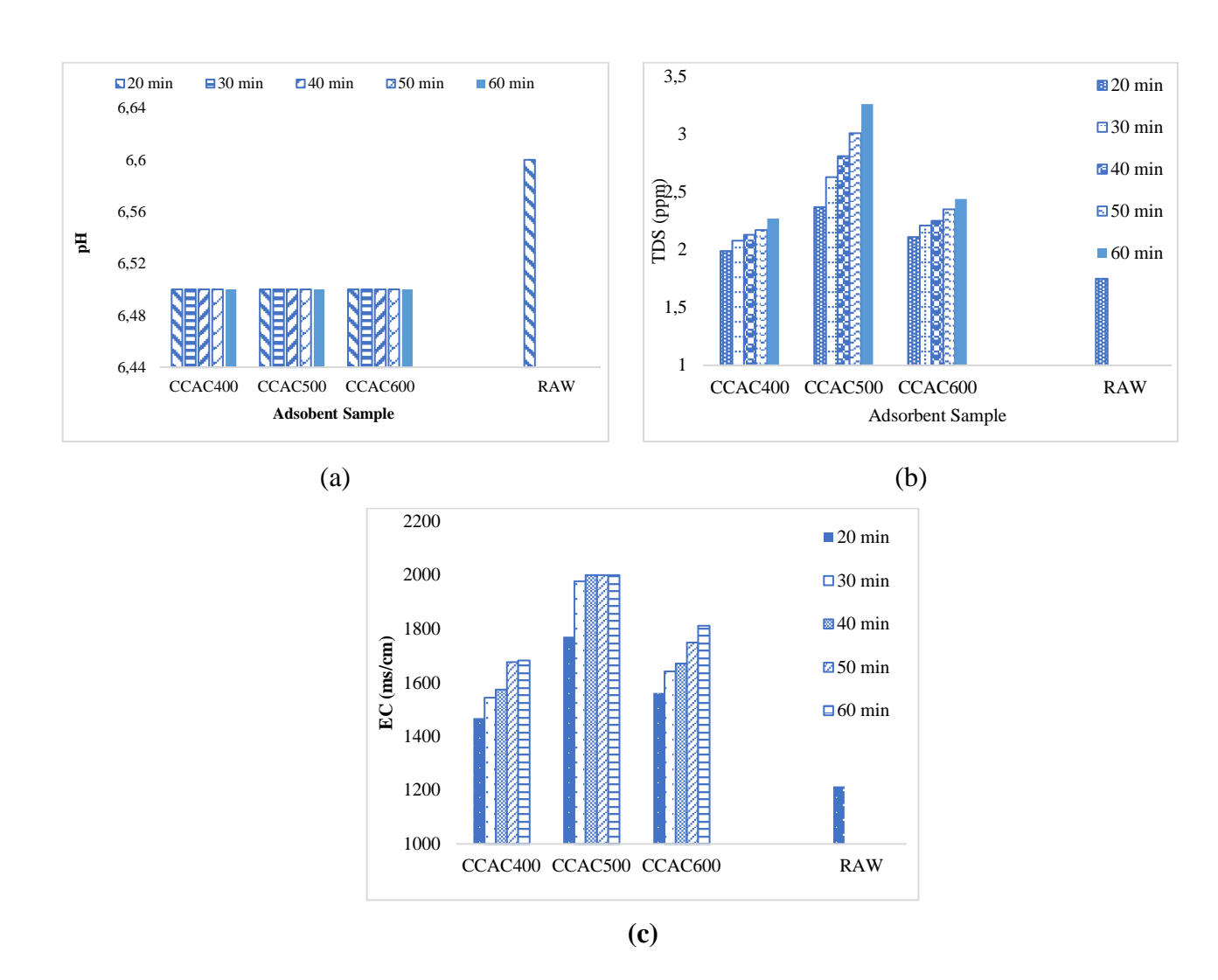


Figure 4: SEM micrograph of (a) CCAC400, (b) CCAC500; (c) CCAC600 at magnification of X1000

The EC observed for water treated with CCAC400, CCAC500 and CCAC600 increased rapidly with the increased retention time (Figure 5c). The highest (2000 mS/cm) and lowest (1214 mS/cm) EC were recorded at 60 mins for CCAC500 and 20 mins for CCAC500, respectively. The higher the concentration of the dissolved charged chemicals, such as salts, in the water, the greater the electrical current that can be conducted. The water standards are compared with the water samples used in this research (Table 6).

## 2.4 Radon Concentration in water samples

All the water sample sources tested (Table 7) had radon concentrations above the maximum contaminant level (0.1 Bq/L) given by SON, however, the sample from the Basic School had the highest radon concentration (31.60 Bq/L), which is above the maximum contaminant level (11.1 Bq/L) suggested by USEPA.



**Figure 5:** (a) pH values, (b) Total dissolved solids and (c) Electrical conductivity of the raw and treated water sample

**Table 6:** Water standards

Samples	Selected Physicochemical Characteristic			
	pН	TDS (ppm)	EC (mS/cm)	
Raw	6.6	1.75	1214	
CCAC400 Treated	6.5	1.99	1682	
CCAC500 Treated	6.5	2.37	2000	
CCAC600 Treated	6.5	2.11	1812	
WHO & SON	6.5-8.5	1000	500	

	1 7
Sampling location	Radon concentration (Bq/L)
Palace	1.69
Ile Ojude	1.09
Orire LG secretariat	6.51
Ile Olomoba	1.36
Omo Ola aluminium	1.26
Health Centre	6.33
Basic School	31.60

**Table 7:** Radon Concentration in water samples in Ikoyi

## 2.5 Effect of Carbonized Temperature and Contact Time on Adsorption of Radon

The CCAC400, CCAC500 and CCAC600 reduced the radon concentrations in the water samples from 20.06 to 5.15 Bq/L, 4.17 Bq/L and 6.54 Bq/L, respectively, within the time range 20-60 mins (Figure 6a). This led to maximum Percentage Removal of 74.34, 79.23 and 85.56 %, respectively. Higher carbonization temperature led to higher Removal Efficiency; thus, it can be deduced that the activation temperature influences the effectiveness of the adsorbent produced. The adsorption capacity curve of the CCAC samples produced indicated rapid adsorption within the first 20 mins (Figure 6b) and this suggests the pores of the CCACs were rapidly filled within the period. The trend later became relatively constant, thus with the fewer available sites the force of attraction reduced and the radon rate of attachment to the surface reduced (Okeowo *et al.*, 2020).

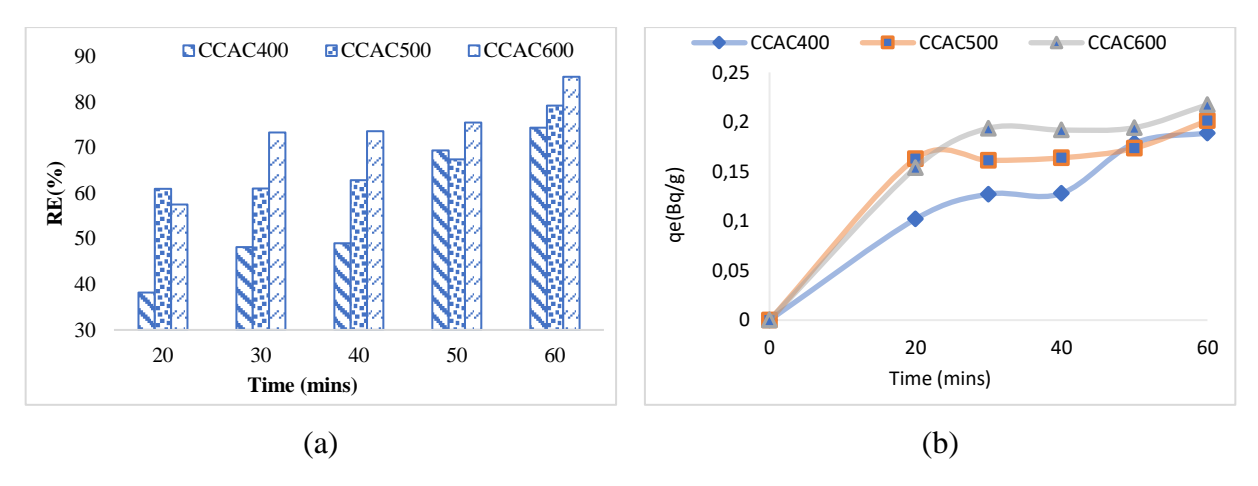


Figure 6: (a) Removal efficiency and (b) Adsorption Capacity of CCAC

## 2.6 Investigation of Kinetic Models

The kinetic data obtained from this study was tested by the use of Pseudo-first order, Pseudo-second order kinetics and Elovich models respectively.

#### 2.6.1 Pseudo-first-order kinetic model

The plot of log ( $q_e$ - $q_T$ ) against time (t) (Figure 7a) was used to evaluate the Pseudo first-order kinetic model constants ( $K_1$  and  $q_e$ ) (Table 8). The Coefficient of Determination ( $R^2$ ) values of the plot exhibit the level of disparity in the data obtained from one another. The  $R^2$  obtained for CCAC400, CCAC500 and CCAC600 were 0.7234, 0.6715 and 0.6945, respectively, and are low relatively (Amole *et al.*, 2021). The estimated first order rate constant  $k_1$  value (0.0392 min<sup>-1</sup>) was higher for CCAC400 while CCAC500 and CCAC600 have the same value of 0.0378 min<sup>-1</sup>. The  $q_e$  calculated values are not close to the  $q_e$  experimental as expected to ascertain the suitability of the model (Strkalj and Malina, 2011). Therefore, based on this, it can be suggested that pseudo-first-order kinetics is not a good fit for this study (Okeowo *et al.*, 2020; Simonin *et al.*, 2016).

#### 2.6.2 Pseudo-second order kinetic model

The values of K<sub>2</sub>, q<sub>e</sub> calculated and R<sup>2</sup> obtained from the plots (Figures 7b-f) of the five resolutions (models) of the pseudo-second-order kinetics models are stated in Table 8. The highest values of K<sub>2</sub> (0.5800, 1.6180 and 1.2610 g/mg.min) were obtained for CCAC400, CCAC500 and CCAC600 with Model I, Model II and Model II, respectively, while the lowest values of K<sub>2</sub> (-0.4101, -5.4880 and -1.4480 g/mg.min) were obtained with Model IV, for all. The q<sub>e</sub> calculated for CCAC400, CCAC500 and CCAC600 were 0.1970, 0.1925 and 0.2160 mg/g, respectively. These values are very close to the q<sub>e</sub> experimental (0.1889, 0.2013 and 0.2174 mg/g) and this further suggested the suitability of the Model II version of the pseudo-second-order kinetics models (Okeowo *et al.*, 2019; Errich *et al.*, 2021; Akartasse *et al.*, 2022a & 2022b). The R<sup>2</sup> (0.8450, 0.9705 and 0.9770) for Model II is relatively the highest. Models I, IV and V are not suitable due to the negative values reported for their K<sub>2</sub>.

#### 2.6.3 Elovich model

The Elovich constants evaluated from the plot of lnqe against  $\ln t$  (Figure 7g) are listed in Table 8. Essentially, the  $R^2$  (0.8726, 0.5613 and 0.8295) obtained for the CCAC400, CCAC500 and CCAC600 respectively, are lower than the  $R^2$  observed for the Model II version of the pseudo-second-order kinetics model, thus the Elovich is not as suitable as pseudo-second-order kinetics model.

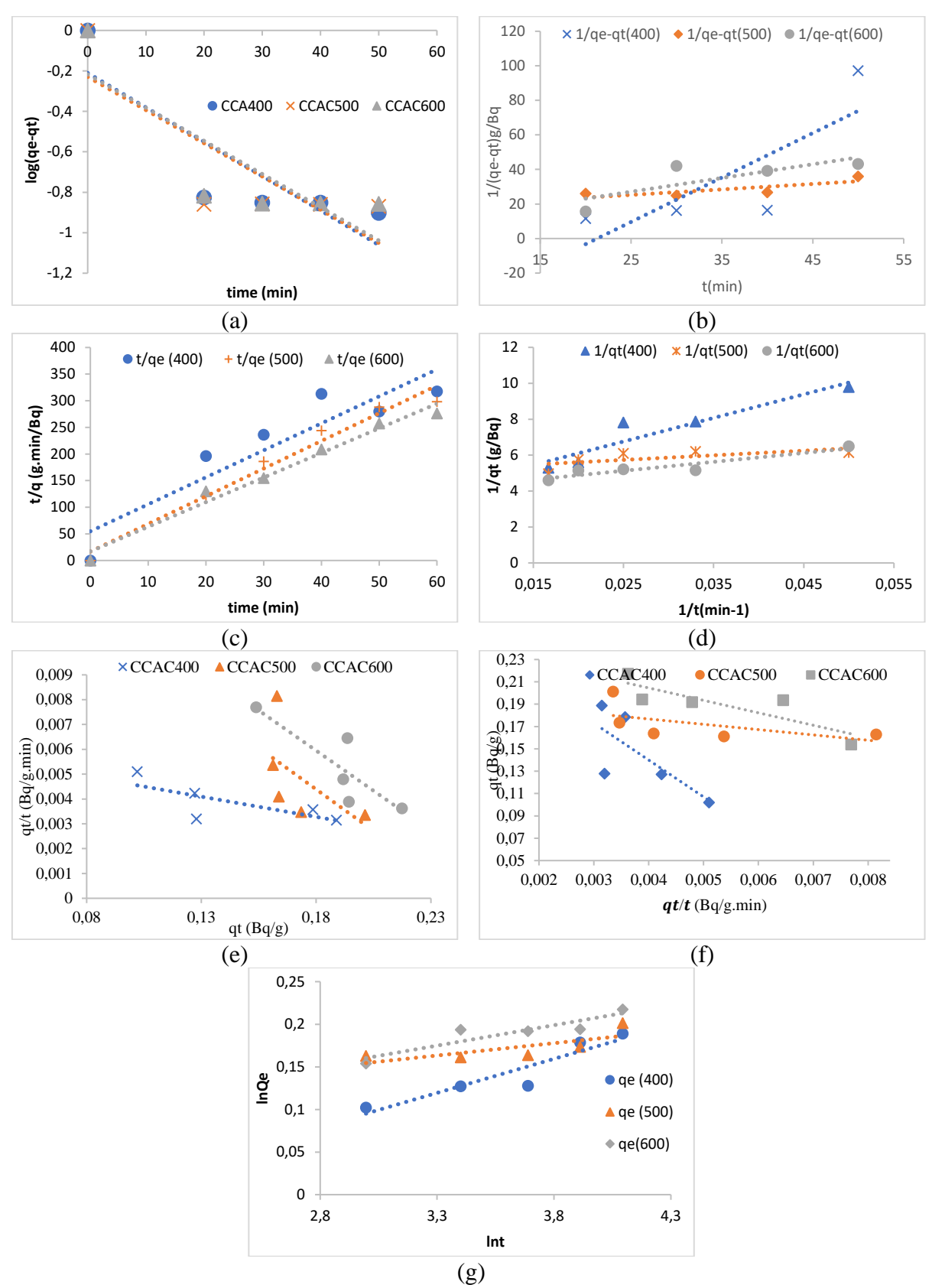


**Figure 7:** (a) pseudo-first-order kinetics plot of  $\log(q_e-q_t)$  vs. time (min) and well as Pseudo-second order (b) (Model I) plot of  $\frac{1}{q_e-q_t}$  against time, (c) (Model II) plot of t/q against time (min), (d) (Model III) plot of 1/qt against 1/t, (e) (Model V) plot of qt/t against qt (f) (Model IV) plot of qt against  $\frac{q_t}{t}$  and Elovich kinetic plot of lnqe vs. ln t.

Model CCAC400 CCAC500 CCAC600 **Parameters** 0.1889 0.2013 0.2174  $q_{e(cal)}(mg/g)$ Pseudo-first order  $K_1 (min^{-1})$ 0.0392 0.0378 0.0378 0.6062  $q_e (mg/g)$ 0.6160 0.6003  $\mathbb{R}^2$ 0.7234 0.6715 0.6945 Pseudo-second 0.5800 -0.4108 -0.3038 $K_2(g/(mg.min))$ order (MOD I) qe(mg/g)0.9718 0.0255 0.0249  $\mathbb{R}^2$ 0.6462 0.6355 0.6242 Pseudo-second  $K_2(g/(mg.min))$ 0.4700 1.6180 1.2610 order (MOD II) 0.1970 0.1925 0.2160 $q_e (mg/g)$ 0.9705 0.9770 0.8450 Pseudo-second  $K_2(g/(mg.min))$ 0.0919 1.0170 0.3050 (MODIII) 0.2570 0.2880 0.1960  $q_e (mg/g)$ 0.8885 0.4371 0.8786 Pseudo-second  $K_2(g/(mg.min))$ -0.4101 -5.4880 -1.4480order (MODIV) 0.2491 0.2719 0.1958  $q_e (mg/g)$ 0.5371 0.3183 0.7205 Pseudo-second  $K_2(g/(mg.min))$ -0.0429 -0.2730 -0.2340order (MOD V) 0.2450 0.2770  $q_e (mg/g)$ 0.3800  $\mathbb{R}^2$ 0.5371 0.3183 0.7205 Elovich  $\propto (g/(mg.min))$ 0.3922 0.1840 0.0451 12.516 34.483 20.833  $\beta$  (mg/g)  $\mathbb{R}^2$ 0.8726 0.5613 0.8295

**Table 8:** The fitting parameters of adsorption kinetics

## 2.7 Error Analysis

The Sum of the Square of The Errors (SSE), Sum of the Absolute Errors (SAE), and Average Relative Error (ARE) to find out the best-fit isotherm model for the experimental equilibrium data are presented in Table 9.

**Error** Adsorbent **Kinetic Models** analysis **PFO** PSO I **PSO II PSO IV** PSO V **PSO III** CCAC400 6.9327 17.094 0.0678 0.5119 0.4032 1.38184 SSE CCAC500 4.5745 0.5404 0.0099 0.0137 0.1312 0.0135 CCAC600 4.3268 0.6829 0.1116 0.0867 0.1884 0.0166 CCAC400 2.633 4.1345 0.2605 0.7155 0.635 1.1755 SAE CCAC500 2.1388 0.7351 0.0998 0.1173 0.3623 0.1163 CCAC600 2.0801 0.8263 0.1291 0.3341 0.2946 0.4341 CCAC400 502.02 607.08 43.337 109.54 97.834 176.48 **ARE** CCAC500 12.34 14.382 14.266 42.978 500.64 85.118 CCAC600 501.17 86.74 15.026 36.86 32.653 47.51

**Table 9:** Error analysis

The SSE obtained for CCAC400, CCAC500 and CCAC600 are in the ranges 0.06787-17.09424, 0.009965-4.57458, and 0.016669 where the minimum SSE was obtained at PSOII. The SAE obtained

for CCAC400, CCAC500 and CCAC600 are in ranges 0.2605-4.1345, 0.0998-2.1388 and 0.1291-2.0801, where PSOII had the lowest SAE error. The ARE obtained for CCAC400, CCAC500 and CCAC600 are in ranges 43.3371-607.08, 12.3404-500.64 and 15.026-501.17 where PSOII had the lowest ARE. The CCAC400 had the highest SSE, SAE and ARE at PSOI, while Pseudo second-order Model II had the lowest error for SSE, SAE and ARE.

## 2.8 Diffusion mechanism models

Intraparticle diffusion model (Webber Morris model), Dumwald-Wagner model and McKay film diffusion mass transfer were used in determining the diffusion mechanism of the biosorption process. The plots for the models are shown in Figures 8a-c.

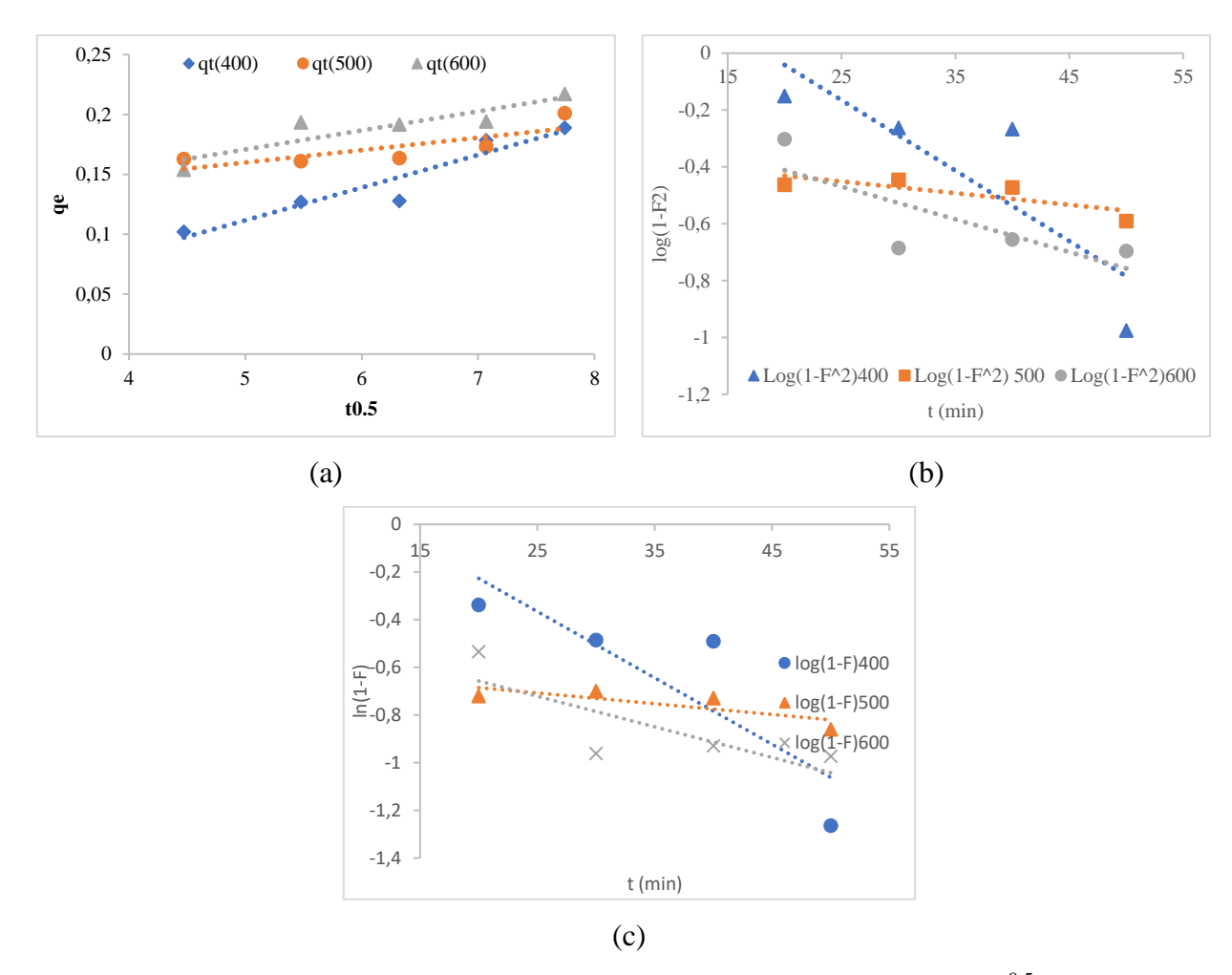


**Figure 8:** (a) Intraparticle diffusion (Webber-Morris) model plot of qe against t<sup>0.5</sup>, (b) Dumwald-Wagner diffusion model plot of log (1-F<sup>2</sup>) against time and (c) McKay film diffusion model plot of ln (1-F) against time

The estimated Webber & Morris rate constant estimated from the plot  $(k_{id})$  is 0.0273, 0.0103 and 0.0159 mg/g/min- $^{1/2}$ , while the external surface (A) is 0.024, 0.1082 and 0.0914 m<sup>2</sup>/g for CCAC400, CCAC500 and CCAC600 respectively, (Table 10), while their R<sup>2</sup> values are 0.9019, 0.6346 and 0.8068 respectively

with the highest value at CCAC400 while CCAC500 had the lowest value as against the trend repeated in Dumwald-Wagner and McKay. These values are in the same range (0.00483-0.137) as (Byungryul, 2020) when he worked on the adsorption of Cu(II) and As(V). Webber & Morris had the highest R<sup>2</sup> values (0.9019, 0.6346 and 0.8068) compared with Dumwald-Wagner and McKay. The Dumwald-Wagner plot did not give excellent R<sup>2</sup> values (0.7158, 0.6377 and 0.6180) as much as the R<sup>2</sup> values (0.7357, 0.6380 and 0.6173) for the McKay film diffusion mass transfer rate model.

Model	Parameters	AC400	AC500	AC600
Webber & Morris	$K_i (mg/g/min-^{1/2})$	0.0273	0.0103	0.0159
	A (Intercept)	0.0240	0.1082	0.0914
	$\mathbb{R}^2$	0.9019	0.6346	0.8068
Dumwald Wagner	$K_{DW}$ (1/min)	-0.0094	-	-1.6230
			1.6247	
	$\mathbb{R}^2$	0.7158	0.6377	0.6180
McKay	$K_{M}$ (1/min)	0.0010	-	-0.0106
			0.0128	
	$\mathbb{R}^2$	0.7357	0.6380	0.6173

**Table 10:** The fitting parameters of Mass Transfer Models

#### **Conclusion**

This project attempts to identify and study activated corncob as an efficient and effective adsorbent for the removal of Radon from water and also to compare the carbonization temperatures of the corncob and retention time in the adsorption efficiency. These adsorbents pose advantages that are of economic value, generate zero waste and are eco-friendly as they utilise the waste by-products which is abundant in nature. FTIR spectra analysis for the corncob sample and activated carbon (AC) sample showed the presence of O-H, C-H, C=O, C-O, C-OH, C-Br, C=C and C-F functional groups which influence enhancement in adsorption abilities of activated carbon onto the adsorbent. SEM images of the CCAC400, CCAC500 and CCAC600 samples showed the surface texture and porosity with holes and small openings found on the surfaces which facilitate pore diffusion of adsorbate during adsorption.

The reduction of Radon concentration at 74 %, 79 % and 86 % at 60 mins, based on the CCAC at 400 °C, 500 °C and 600 °C, respectively, indicates that the activation temperature played a major role in the adsorption capacity. The higher the carbonized temperature, the higher the adsorption capacity of the corncob activated. It was also observed that the Pseudo-second order model II best describes the adsorption capacity of the corncob. The pseudo-second-order model II adsorption kinetics has shown to

be best fitted in describing the adsorption kinetics of the corncob as it had the lowest error. This indicates that the adsorption process is dominated by chemical adsorption. Webber-Morris diffusion model is the best fit for adsorption diffusion. This research identified activated corncob carbonized at 600°C as an efficient and effective adsorbent for the removal of Radon from water. The potency and effectiveness of CCAC as adsorbents for the remediation of radon concentration in groundwater have been established.

#### **Conflict of Interest**

The authors declare that the research was conducted in the absence of any commercial or financial relationships that could be construed as a potential conflict of interest.

#### References

- Abubakar, U., Yusuf, K., Safiyanu, I., Abdullahi, S. Saidu, S., Abdu, G. and Indee, A. (2016). Proximate and mineral composition of corn cob, banana and plantain peels. *International Journal of Food Science and Nutrition*. 1 (6): 25-27.
- Adabanija M., Afolabi A., Olatunbosun A., and Kolawole L., (2014). Integral approach to investigation of occurrence and quality of groundwater in Ogbomoso North, Southwestern Nigeria. *Environmental Earth Sciences*. 73:139-162
- Adagunodo T., Sunmonu L., Oladejo O. and Olafisoye E. (2013). Ground Magnetic Investigation into the Cause of the Subsidence in the Abandoned Local Government Secretariat, Ogbomoso, Nigeria. *ARPN Journal of Earth Sciences*, 2(3), 101–109.
- Aeration Process for Removing Radon from Drinking Water -A Review. Available from: https://www.researchgate.net/publication/333748175\_Aeration\_Process\_for\_Removing\_Radon\_from\_Drinking\_Water\_-A\_Review [accessed Feb 16, 2022].
- Akartasse N., Azzaoui K., Mejdoubi E., Elansari L. L., Hammouti B., Siaj M., Jodeh S., Hanbali G., Hamed R., Rhazi L. (2022a), Chitosan-Hydroxyapatite Bio-Based Composite in film form: synthesis and application in Wastewater, *Polymers*, 14(20), 4265, https://doi.org/10.3390/polym14204265
- Akartasse N., Azzaoui K., Mejdoubi E., Hammouti B., *et al.* (2022b), Environmental-Friendly Adsorbent Composite Based on Hydroxyapatite/Hydroxypropyl Methyl-Cellulose for Removal of Cationic Dyes from an Aqueous Solution, *Polymers*, 14(11), 2147; https://doi.org/10.3390/polym14112147
- Akuso, S., Abubakar, G., Nwobi, B., Abdullahi, M., Ayilara, S., Batari, M. and Umar, M. (2019). Production and Characterization of Activated Carbon (AC) from Corncob for Methylene Blue and Chromium (Vi) Adsorption. *Nigerian Research Journal of Chemical Sciences*, 6:1-13.
- Alabdula'aly A. and Maghrawy H. (2011). Comparative study of different types of granular activated carbon in removing medium-level radon from water. *Journal of Radioanalytical and Nuclear Chemistry* 287:77-85
- Amodu, F. Faluyi, O. Ben, F. and Edaogbogun, G. (2020). Assessment of Radiological Risk of Radon in Borehole Water in Ede and its Environs. *Global Scientific Journals*. 8(5):486-502.

- Amole, A.R., Araromi, D.O., Alade, A.O., TJ Afolabi, VA Adeyi (2021). Biosorptive removal of nitrophenol from aqueous solution using ZnCl<sub>2</sub>-modified groundnut shell: optimization, equilibrium, kinetic, and thermodynamic studies. *Int. J. Environ. Sci. Technol.* (2020). https://doi.org/10.1007/s13762-020-02939-y
- Amuda, O.S., Adebisi, S.A., Jimoda, L.A., and Alade, A.O. (2014). Challenges and Possible Panacea to the Municipal Solid Wastes Management in Nigeria. *Journal of Sustainable Development Studies*. 6 (1): 64-70
- Anih, E., Babarinde, O., and Adeyemi, M., (2020). Adsorptive Efficiency of Activated Carbon from Corncob compared with commercial Activated Carbon in the Adsorption of Light Alkanes Contaminant in Hydrogen Gas Product. *Chemical Science International Journal*, 29(2): 11-24
- Appleton, J. (2007). Radon: Sources, Health Risks, and Hazard Mapping. *AMBIO: A Journal of the Human Environment*, 36(1):85–89.
- Arora V, Bajwa B S and Singh S (2011). Measurements of radon concentrations in groundwater samples of tectonically active areas of Himachal Pradesh, North West Himalayas, *India Radiat Prot Environ* 34 50–4
- ASTM, (2006), Standard Test Method for determination of iodine number for activated carbon. ASTM Committee on stands. ASTMO 4607-94 Philadelphia, P.A.
- Bryant, I. and Tettehh-Narh, R. (2015). Using Slow Sand Filtration System with Activated Charcoal layer to treat Salon Wastewater in a Selected Community in Cape Coast, Ghana. *Journal of Advanced Chemical Engineering*. 5(4):1-8.
- Byungryul, A. (2020). Cu(II) and As(V) Adsorption Kinetic Characteristic of the Multifunctional Amino Groups in Chitosan. *Processes*. 8:1-15
- Choubey VM, Bartarya SK, Saini NK and Ramola RC (2001) Radon measurements in groundwater of inter-montane Doonvalley, Outer Himalaya: effects of geohydrology and neotectonic activity. Environ Geol 40(3):257–266
- Danert, K. and Healy, A. (2021). Monitoring Groundwater Use as a Domestic Water Source by Urban Households: Analysis of Data from Lagos State, Nigeria and Sub-Saharan Africa with Implications for Policy and Practice. *Water* 13: 1-18
- Durridge Radon Instrumentation RADH<sub>2</sub>O User Manual (2016). Available online at: https://www.durridge.com/documentation/rad%20H2020% manual.pdf.
- Dvorak, B. and Skipton, S. (2013). Drinking-Water Treatment: Activated Carbon Filtration. *Nebguide G1489* http://extension.unl.edu/publications/g1489
- Ekpete, O. and Horsfall, M. (2011). Kinetic Sorption Study of Phenol onto Activated Carbon Derived from Fluted Pumpkin Stem Waste (*Telfaria occidentalis Hook F*). *ARPN Journal of Engineering and Applied Sciences*. 6 (6):43-49
- Elmorsi, T., Mohamed, Z., Shopak, W. and Ismaiel, A. (2014). Kinetic and Equilibrium Isotherms Studies of Adsorption of Pb(II) from Water onto Natural Adsorbent. *Journal of Environmental Protection*, 5: 1667-1681.

- EPA (2003). Environmental Protection Agency. Assessment of risks from radon in homes, Office of Radiation and Indoor Air United States Environmental Protection Agency Washington DC
- EPA (2014). United States Environmental Protection Agency, Basic Information about Radon in Drinking Water. from https://archive.epa.gov/water/archive/web/html/basicinformation-2.html
- EPA (United States Environmental Protection Agency) (1999) Radon in drinking water health risk reduction and cost analysis, Vol 64. Federal Register, Washington, pp 9559–9599
- Errich A., Azzaoui K., Mejdoubi E., Hammouti B., Abidi N., Akartasse N., Benidire L., EL Hajjaji S., Sabbahi R., Lamhamdi A. (2021), Toxic heavy metals removal using a hydroxyapatite and hydroxyethyl cellulose modified with a new Gum Arabic, *Indonesian Journal of Science & Technology*, 6(1), 41-64
- EU (2001). European Union Commission Recommendation on the protection of the public against exposure to radon in drinking water supplies. *Office Journal of the European Community*, 344: 85-88.
- EU (2013) European Union Council Directive 2013/51/Euratom of 22 October 2013 laying down requirements for the protection of the health of the general public with regard to radioactive substances in water intended for human consumption Web: <a href="http://eur-lex.europa.eu/legal-content/EN/TXT/?uri=CELEX:32013L0051">http://eur-lex.europa.eu/legal-content/EN/TXT/?uri=CELEX:32013L0051</a>
- Ezeh, E., Okeke, O., Abura, C., Aniobi, C., Ndubuisi, J. (2019). Adsorption Efficiency of Activated Carbon Produced from Corncob for the Removal of Cadmium Ions from Aqueous Solution. *International Journal of Advanced Research in Chemical Science*. 6(7):14-22.
- Fapetu O. (2000). Production of Charcoal from Tropical Biomass for Industrial and Metallurgical Processes. *Nigerian Journal of Engineering Management* 1(2):34-37
- Feng, Y., Yang, W., & Chu, W. (2015). Contribution of Ash Content Related to Methane Adsorption Behaviors of Bituminous Coals. *International Journal of Chemical Engineering*, 1(5), 1-11.
- Feriz Adrovic, Intech Open. https://www.intechopen.com/books/radon/radon-nuclides-and-radon-generators
- Ghernaout Djamel (2019) Aeration Process for Removing Radon from Drinking Water A Review. Applied Engineering. 3(1):32-45. doi: 10.11648/j.ae.20190301.15
- Guppy, L.; Uyttendaele, P.; Villholth, K.G.; Smakhtin, V. (2018) Groundwater and Sustainable Development Goals: Analysis of Interlinkages; UNU-INWEH Report Series, Issue 04; United Nations University Institute for Water; Environment and Health: Hamilton, ON, Canada,
- Hu, H., Liang, W., Zhang, Y., Wu, S., Yang, Q., Wang, Y., Liu, Q. (2018). Multipurpose Use of a Corncob Biomass for the Production of Polysaccharides and the Fabrication of a Biosorbent. ACS Sustainable Chemistry & Engineering, 6(3), 3830-3839.
- Hubbe, M. (2021). Insisting upon Meaningful Results from Adsorption Experiments. *Sep. Purif. Rev.* 1–14
- Idriss, H., Salih, I., & Sam, A. K. (2011). Study of radon in groundwater and physicochemical parameters in Khartoum state. Journal of Radioanalytical and Nuclear Chemistry, 290(2), 333–338. doi:10.1007/s10967-011-1295-4

- Igwegbe, C., Umembamalu, C., Osuaqwu, E., Oba, S. and Emembolu, L. (2021). Studies on Adsorption Characteristics of Corncobs Activated Carbon for the removal of oil and grease from Oil Refinery Desalter Effluent in a Down Flow Fixed Bed Adsorption Equipment. *European Journal of Sustainable Development Research*. 5(1):1-14.
- Jeandson, C., Roberta, N., Marcio, A. M., & Dênia, M. D. (2018). The oven-drying method for determination of water content in Brazil nut. *Bioscience Journal*, 34(3), 595-602.
- Justyna K. (2012). Sorption Properties of Activated Carbons Obtained from Corncobs by Chemical and Physical Activation. *Adsorption*. 19:273-281.
- Kajjumba, G., Öngen, H., and Özcan, S. (2018). Modelling of adsorption kinetic processes Errors, Theory and Application. http://dx.doi.org/10.5772/intechopen.80495
- Kundu, S. and Gupta, A. (2006). Arsenic adsorption onto iron oxide coated cement (IOCC): regression analysis of equilibrium data with several isotherm models and their optimization. *Chemical Engineering Journal*, 122(2): 93–106.
- Lowry, J. and Lowry, S. (1988). Radionuclides in Drinking Water. *American Water Works Association Journal*. 80:51-64.
- Malik, R., Ramteke, D. and Wali, S. (2007). Adsorption of Malachite green on groundnut shell waste-based powdered activated carbon. *Journal of Waste Management and Disposal*. 27:1129-1138.
- Muikku M., Heikkinen T., Puhakainen M., Rahola T. and Salonen L (2007). Assessment of occupational exposure to uranium by indirect methods needs information on natural background variations. *Journal of Radiation Protection Dosimetry* 125:492-495
- Mustafa, A. and Daniel, K. (2009). Health effects of radon: A review of the literature. *International Journal of Radiation Biology*, 1:57-69
- N'diaye A.D., Kankou M.S.A., Hammouti B., Nandiyanto A.B.D., Al Husaeni D.F. (2022). A review of biomaterial as an adsorbent: From the bibliometric literature review, the definition of dyes and adsorbent, the adsorption phenomena and isotherm models, factors affecting the adsorption process, to the use of typha species waste as adsorbent. *Communications in Science and Technology*, 7(2), 140-153. https://doi.org/10.21924/cst.7.2.2022.977
- Okeowo, I.O., Balogun, E.O., Ademola, A.J., Alade, A.O., Afolabi, T.J., (2020). Adsorption of Phenol from Wastewater Using Microwave-Assisted Ag–Au Nanoparticle-Modified Mango Seed Shell-Activated Carbon. *Int J Environ Res* 14, 215–233. https://doi.org/10.1007/s41742-020-00244-7t
- Olaoye, R. A., Afolayan, O. D., Mustapha, O. I. and Adeleke, H. G. (2018a). The Efficacy of Banana Peel Activated Carbon in the Removal of Cyanide and Selected Metals from Cassava Processing Wastewater, *Advances in Research*, 16 (1): 1-12.
- Olaoye, R.A, Coker, A.O., Sridhar M.K.C. (2021) Variation of Groundwater and Rainwater Quality in a Nigerian Leper Colony, *European Journal of Advanced Chemistry Research*, 2(3), 27 33.
- Olaoye, R.A, Ojoawo, S.O, Oluremi, J.R and Yusuf, A.D (2018). Pilot Study on Low-Cost Domestic Slow Sand Filter for Groundwater Quality Improvement, *LAUTECH Journal of Engineering and Technology (LAUJET)*, 12(1):43-52

- Olaoye, R.A., Oladeji, O.S., Olaniyan, O.S. and Salami, M. O. (2018). Remediation of Textile Wastewater Using Activated Rice Husk, *IOSR Journal of Engineering* (IOSRJEN), 8 (6): 8 -15.
- Oni, E., Oni, O., Oladapo, O., Olatunde, I. and Adediwura, F. (2016). Measurement of Radon Concentration in Drinking Water of Ado-Ekiti, Nigeria. *Journal of Academia and Industrial Research (JAIR)* 4(8):190-192
- Oni, M., Oladapo, O., Amuda, D., Oni, E., Adelodun, A., Adewale, Y. and Fasina, M. (2014). Radon concentration in groundwater areas of high background radiation level in Southwestern Nigeria. *Nigeria Journal of Physics*. 25(1): 64-67.
- PWS (2019). Private Water Supplies Sampling Procedures Manual Version 1.5 (2019) http://dwi.defra.gov.uk/private-water-supply/regs-guidance/Guidance/sampling/pws-sampling-procedures.pdf
- Qui, Y., Cheng-C, X. and Shengi, S. (2008). Surface Characterization of crop residue-derived black carbon and lead (II) adsorption, *Journal of Water Resources*. 42:567-574
- Rao, M., Roddy, D., Venkateswarth, P. and Seshaiah, K. (2009). Removal of Mercury from aqueous solutions using activated carbon prepared from agricultural by-product-waste. Journal of Environ Manage. 90(1):634-643.
- Sabino, D., Giusy L., Mariangela G., Michele, L. (2016). Characteristics and Adsorption Capacities of Low-Cost Sorbents for Wastewater Treatment: A Review. *Sustainable Materials and Technologies*. 9:10-40.
- Seminsky, K. and Seminsky, A. (2016). Radon in Underground Waters of Baikal and Transbaikalia: Spatialtemporal Variations. *Geodynamics and Tectonophysics*, 7(3), 477-493.
- Sharma, A., Tomer, A., Singh, J., and Chhikara, B. S. (2019). Biosorption of metal toxicants and other water pollutants by corn (maize) plant: A comprehensive review. *Journal of Integrated Science and Technology*, 7(2), 19-28.
- Simonin J-P. (2016), On the comparison of pseudo-first order and pseudo-second order rate laws in the modeling of adsorption kinetics, *Chemical Engineering Journal*, 300, 254-263, ISSN 1385-8947, https://doi.org/10.1016/j.cej.2016.04.079
- SON (2007). Nigeria Standard for drinking water. Standards organization of Nigeria. NIS554:2007
- Strkalj, A. and Malina, J. (2011). Thermodynamic and Kinetic study of Ni (ii) Ions on Carbon Anode Dust. *Journal of Chemical Engineering Communications*, 198:1497-1504
- Sunmonu, L., Adagunodo, T., Olafisoye, E. and Oladejo O. (2012). The Groundwater Potential Evaluation at Industrial Estate Ogbomoso Southwestern Nigeria. *RMZ-Materials and Geoenvironment*, 59(4):363–390.
- Sunmonu, L., Olafisoye, E., Adagunodo T. and Alagbe O. (2013). Geophysical and Hydrophysicochemical Evaluation of Hand-dug Wells near a Dumpsite in Oyo State, Nigeria. *Archives of Applied Science Research*, 5(6), 29–40.
- U.S. Environmental Protection Agency. National primary drinking water regulations. Washington, DC: EPA; (2009). Available from: http://water.epa.gov/drink/contaminants/index.cfm#List.

- United States Environmental Protection Agency (1993). Protocols for Radon and Radon Decay Product Measurement in Homes. USEPA Publication 402-R-92-003. Washington, D.C.
- USEPA (1999). Technologies and costs for the removal of radon from drinking water, United States Environmental Protection Agency (USEPA), Office of Water 4607, EPA B15-D99-004, https://nepis.epa.gov/Exe/ZyPDF.cgi/20001XQU.PDF?Dockey=20001XQU.PD
- USEPA (2010). United States Environmental Protection Agency, New Jersey Drinking Quality Institute. (2010). A South Jersey homeowner's guide to radioactivity in drinking water: Radium. Retrieved from www.nj.gov/dep/watersupply/pdf/radium\_bb\_5\_20\_02.pdf
- Webber, W. and Morris, J. (1963). Kinetics of adsorption on carbon from solution. *J. Sanit. Eng. Div.* 89: 31–59.
- WHO (2008). World Health Organization guidelines for drinking water quality. In: Incorporating First and Second Addenda, third ed. WHO Press, Geneva. (2008), 3<sup>rd</sup> ed. World Health Organisation, Geneva, Switzerland.
- World Health Organization (2002). Guidelines for Drinking Water Quality, <a href="http://www.who.int/water\_sanitation\_health/GDWQ/index.html.Geneva">http://www.who.int/water\_sanitation\_health/GDWQ/index.html.Geneva</a>, Switzerland: WHO
- Yang, K., Peng, J., Srinivasakannan, C., Zhang, L., Xia, H. and Duan, X. (2010). Preparation of high surface area activated carbon from coconut shells using microwave heating. *Bioresource Technology*, 101: 6163–6169.
- Yusuf O. (2019). Assessment of Radon exposure from hand-pumped groundwater in Nigeria, Ogbomoso, Southwestern Nigeria. Unpublished M. Tech Dissertation submitted to the Department of Pure and Applied Physics. Ladoke Akintola University of Technology (LAUTECH), Ogbomoso.
- Zhou, Q., Zhaoa, G., Xiaoa, D., Qiua, S., Leic, Q., and Kearfott, K. (2018). Prediction of radon removal efficiency for a flow-through activated charcoal system and radon mitigation characteristics. *Radiation Measurements*. 10 (4)1-20.

(2024); www.mocedes.org/ajcer